A high frequency optical trap for atoms using Hermite-Gaussian beams

T. P. Meyrath, F. Schreck, J. L. Hanssen, C. -S. Chuu, M. G. Raizen

Center for Nonlinear Dynamics and Department of Physics,
The University of Texas at Austin, Austin, Texas 78712-1081, USA

meyrath@physics.utexas.edu

Abstract: We present an experimental method to create a single high frequency optical trap for atoms based on an elongated Hermite-Gaussian TEM_{01} mode beam. This trap results in confinement strength similar to that which may be obtained in an optical lattice. We discuss an optical setup to produce the trapping beam and then detail a method to load a Bose-Einstein Condensate (BEC) into a TEM_{01} trap. Using this method, we have succeeded in producing individual highly confined lower dimensional condensates.

OCIS codes: (020.0020) Atomic and molecular physics; (020.7010) Trapping

References and links

1. M.H. Anderson, J.R. Ensher, M.R. Matthews, C.E. Wieman, and E.A. Cornell, "Observation of Bose-Einstein Condensation in a Dilute Atomics Vapor," Science **269**, 198-201 (1995).
2. K. B. Davis, M. -O. Mewes, M. R. Andrews, N. J. van Druten, D. S. Durfee, D. M. Kurn, and W. Ketterle, "Bose-Einstein Condensation in a Gas of Sodium Atoms," Phys. Rev. Lett. **75** 3969 (1995).
3. Conventional magnetic traps refer to Ioffe-Prichard type or TOP traps, atom chip setups may also generate high strength traps because of the close proximity of the atoms to the chip surface [4].
4. R. Folman, P. Krüger, J. Schmiedmayer, J. Denschlag, and C. Henkel, "Microscoptic Atom Optics: From Wires to an Atom Chip," Adv. At. Mol. Opt. Phys. **48**, 263 (2002).
5. P. S. Jessen and I. H. Deutsch, "Optical Lattices," Adv. At. Mol. Opt. Phys. **37** 95-138, 1996.
6. M. Greiner, O. Mandel, T. Esslinger, T.W. Hänsch, Immanuel Bloch, "Quantum phase transition from a superfluid to a Mott insulator in a gas of ultracold atoms," Nature **415**, 39 (2002).
7. B. Paredes, A. Widera, V. Murg, O. Mandel, S. Fölling, I. Cirac, G.V. Shlyapnikov, T.W. Hänsch, I. Bloch, "Tonks-Girardeau Gas of Ultracold Atoms in an Optical Lattice," Nature **429**, 277 (2004).
8. T. Kinoshita, T. Wenger, and D.S. Weiss, "Observation of a One-Dimensional Tonks-Girardeau Gas," Science **305**, 1125 (2004).
9. B. Laburthe Tolra, K. M. O'Hara, J. H. Huckans, W. D. Phillips, S. L. Rolston, and J. V. Porto, "Observation of Reduced Three-Body Recombination in a Correlated 1D Degenerate Bose Gas," Phys. Rev. Lett. **92**, 190401 (2004).
10. R.B. Diener, B. Wu, M.G. Raizen, and Q. Niu, "Quantum Tweezer for Atoms," Phys. Rev. Lett. **89**, 070401 (2002).
11. Saleh and Teich, *Fundamentals of Photonics*, (Wiley, New York, 1991).
12. The waist sizes depend on the propagation distance s as $W_{q,p}^2(s) = W_{q,p}^2(0) + (\lambda s/\pi W_{q,p}(0))^2$ [11]. This fact results in a weak anti-trap in this direction, see Eq. (8).
13. R. Grimm, M. Weidemüller, and Y.B. Ovchinnikov, "Optical Dipole Traps for Neutral Atoms," Adv. At. Mol. Opt. Phys. **42**, 95 (2000).
14. N. Freidman, A. Kaplan, N. Davidson, "Dark Optical Traps for Cold Atoms," Adv. At. Mol. Opt. Phys. **48**, 99 (2002).
15. MgF_2 was chosen because it is a soft coating and more easily makes a sharp feature. This thickness is for a π relative phase difference at wavelength $\lambda = 532\,\mathrm{nm}$
16. W. Wohlleben, F. Chevy, K. Madison, and J. Dalibard, "An Atom Faucet," Eur. Phys. J. D **15**, 237 (2001).
17. T. Esslinger, I. Bloch, and T.W. Hänsch, "Bose-Einstein condensation in a quadrupole-Ioffe-configuration trap," Phys. Rev. A, Vol. 58, pp. R2664 No 4, (1998).

#6677 - $15.00 US Received 28 February 2005; revised 30 March 2005; accepted 30 March 2005

18. The TEM_{01} traps discussed here use laser wavelength $\lambda = 532$ nm and the infrared vertical trap uses $\lambda = 1064$ nm. These are *blue* and *red* relative to the strong transitions of rubidium near 780 nm. Blue traps result in a repulsive potential whereas red traps result in an attractive potential [13].
19. Yariv and Yeh, *Optical Waves in Crystals*, (Wiley, New York, 1984).
20. This is what it means to be lower dimensional, the motion in the strongly confined direction is frozen out and the wave function may be written as the ground state of a single particle harmonic oscillator in the direction in question. This occurs when the three-dimensional chemical potential μ_{3D} is below the harmonic oscillator energy state splitting of the strong direction $\hbar\omega_q$ [21].
21. D. S. Petrov, G. V. Shlyapnikov, and J. T. M. Walraven, "Regimes of Quantum Degeneracy in Trapped 1D Gases," Phys. Rev. Lett. **85**, 3745 (2000).
22. Y. Castin and R. Dum, "Bose-Einstein Condensates in Time Dependent Traps," Phys. Rev. Lett. **77** 5315 (1996).
23. We use values for the D_2 line of rubidium 87: $I_s \cong 1.67\,\mathrm{mW/cm^2}$, $\Gamma \cong 2\pi \cdot 6.065\,\mathrm{MHz}$, $\omega_0 \cong 2\pi \cdot 384.23\,\mathrm{THz}$, and $m \cong 1.443 \times 10^{-25}\,\mathrm{kg}$. In Eq. (3), it is important not to use the common rotating wave approximation (which is to assume $|\omega_0 - \omega| \ll \omega_0 + \omega$ and neglect the second term in parenthesis) because the detuning is too far for this to be valid. This is a larger effect than explicitly including the D_1 line which is typically done for nearer detunings.
24. This is a gradium index lens with $f/\# = 2.2$.
25. T.P. Meyrath, F. Schreck, J.L. Hanssen, C.-S. Chuu, and M.G. Raizen, "Bose Einstein Condensation in a Box," Phys. Rev. A (to be published), preprint at cond-mat/0503590.
26. N.L. Smith, W.H. Heathcote, G. Hechenblaikner, E. Nugent, and C.J. Foot, "Quasi-2D Confinement of a BEC in a Combined Optical and Magnetic Potential," J. Phys. B: At. Mol. Opt. Phys. **38** 223-235, 2005.

1. Introduction

In recent years there has been much interest in development of strongly confining traps for ultra-cold atoms. Such traps are particularly attractive for the production of lower dimensional Bose-Einstein condensates (BEC). Although condensates were initially produced in magnetic traps [1, 2], optical traps are an attractive alternative due to their flexibility and may be used to generate traps of strength greatly beyond those of conventional magnetic traps [3, 4]. A widely used optical trap of this sort is an optical lattice [5]. Optical lattice experiments have been performed in a wide variety of contexts and may be made of very high strength for the study of some quantum mechanical phenomenon [6, 7, 8, 9]. Lattice traps, despite this capacity, have a limitation. Typically an optical lattice has a spacing of half the laser wavelength — order a few hundred nanometers. Condensates loaded into these traps which are initially of a size greater than 10 μm are typically split into thousands of distinct condensates. This limits the addressability of the individual condensates which is desirable for direct atom statistics study of some states such as the Mott-insulator transition [6] and the Tonks-Girardeau gas regime [7, 8, 9] and required for others such as the proposed quantum tweezer for atoms [10]. We present an optical trap that may be used to enter these regimes, yet it a single site trap and therefore addressable.

2. A Hermite-Gaussian optical dipole trap

Our approach to creating a high frequency trap for a BEC is based on a Hermite-Gaussian TEM_{01} mode beam. This beam profile has the advantage of having a dark line in the center of the profile. For light detuned blue of an atomic transition this provides a strongly confining trap. The intensity of a Hermite-Gaussian TEM_{01} beam is given by [11]:

$$I(q,p) = \frac{P}{\pi W_q W_p} \frac{8q^2}{W_q^2} \exp\left(-\frac{2q^2}{W_q^2} - \frac{2p^2}{W_p^2}\right), \tag{1}$$

in terms of the beam power P and waist sizes [12] W_q and W_p. The coordinates axes q and p are orthogonal to the axis of propagation s and refer to either x, y, or z depending on the beam orientation: $q = y$, $p = z$, and $s = x$ for horizontally and $q = x$, $p = z$, and $s = y$ for vertically

#6677 - $15.00 US Received 28 February 2005; revised 30 March 2005; accepted 30 March 2005

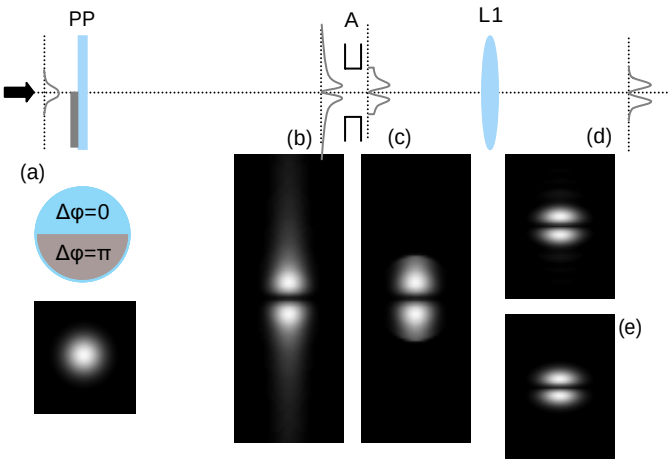

Fig. 1. Optics pictorial showing production of a TEM_{01} from an input Gaussian. (a) An input Gaussian passes the phase plate (PP) giving a relative π phase shift between the halves of the beam. (b) The aperture (A) is in the far field of the output beam from PP. This produces the Fourier transform at A. (c) Higher spatial modes are truncated by A. (d) Lens L1 produces the Fourier transform of the output of A resulting in a near TEM_{01} mode profile. (e) A true TEM_{01} beam, the profile in (d) only deviates in small fringes outside the main lobes. The images are numerically calculated beam profiles shown as $\sqrt{I(q,p)}$.

propagating beams as in Fig. 3. The optical dipole potential for a two-level atom with transition frequency $\omega_0/2\pi$ produced by light of frequency $\omega/2\pi$ with intensity profile $I(q,p)$ is [13, 14]

$$U(q,p) = U_0 \frac{2\mathrm{e}q^2}{W_q^2} \exp\left(-\frac{2q^2}{W_q^2} - \frac{2p^2}{W_p^2}\right), \tag{2}$$

where the central trap depth is given by

$$U_0 = -\frac{\hbar\Gamma^2}{8I_s}\left(\frac{1}{\omega_0-\omega}+\frac{1}{\omega_0+\omega}\right)\frac{4P}{\pi \mathrm{e} W_q W_p}, \tag{3}$$

where Γ is the natural line width of the transition, $I_s = \pi hc\Gamma/3\lambda^3$ is the saturation intensity, and $\mathrm{e} = \exp(1) \cong 2.718$. By expanding Eq. (2) about $q = 0$, the trap oscillation frequency in the q direction inside the TEM_{01} trap can be shown to be

$$\frac{\omega_q}{2\pi} = \sqrt{\frac{\mathrm{e}U_0}{\pi^2 m W_q^2}}, \tag{4}$$

where m is the mass of the atom. From Eq. (4), it is clear that the trap frequency increases with larger power and smaller waist size in the q direction.

A concern with using optical traps is the rate of spontaneous scattering events. Such events lead to heating of the atoms. This rate is given by [13]

$$R(q,p) = \frac{\Gamma^3}{8I_s}\left(\frac{\omega}{\omega_0}\right)^3\left(\frac{1}{\omega_0-\omega}+\frac{1}{\omega_0+\omega}\right)^2 I(q,p). \tag{5}$$

#6677 - $15.00 US
Received 28 February 2005; revised 30 March 2005; accepted 30 March 2005

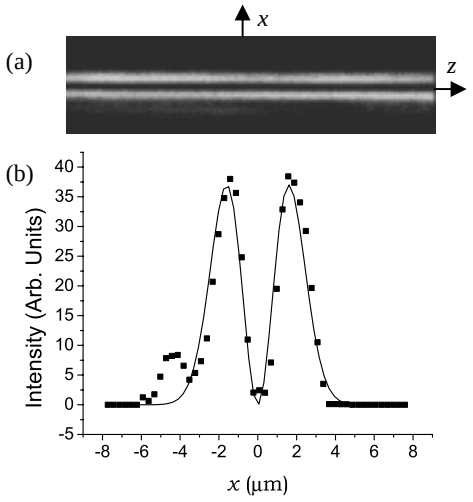

Fig. 2. Profile of TEM_{01} mode beam. (a) A CCD picture of a TEM_{01} trapping beam imaged as seen by the atoms. The image extends only $100\,\mu$m in the z direction. (b) The profile along the narrow axis, the boxes are points integrated along the z axis for the center $10\,\mu$m and the solid line is a fit to an ideal TEM_{01} mode profile in Equation 1, giving a waist size of $W_x = 1.8\,\mu$m.

In a beam of intensity given by Eq. (1), $I(0,p)$ vanishes, but the scattering rate may be estimated by calculating it at the harmonic oscillator length $a_q = \sqrt{\hbar/m\omega_q}$. The rate is low because of the very large detuning used, typically there are few events during the optical trap time.

3. Experimental methods and results

3.1. Hermite-Gaussian beam production

Although it is possible to have a laser directly output a non-Gaussian beam, we use a simple holographic method to produce the TEM_{01} mode beams which are used for the optical trap. The concept is illustrated in Fig. 1. The input Gaussian beam passes a coated phase plate which produces a relative π phase difference between two halves of the beam. This eliminates the Gaussian component of the beam and leaves it as some superposition of the higher modes. Because higher spatial frequencies correspond to larger angles, they are filtered by the aperture which truncates the large wings of the beam. This output is then imaged to produce a nearly TEM_{01} profile. In Fig. 1(e) a true TEM_{01} profile is shown along side the output of the optical system (d) which is very similar save a few small fringes.

The phase plate consists of a standard BK7 double-sided anti-reflection coated window which has an additional coating on one side. The coating is a 6900Å thick MgF_2 layer that extends along half of the face with a sharp straight line boundary [15]. The windows we have used were masked and coated in a vapor deposition machine. The plate takes an input Gaussian mode beam which is aligned as to intersect the plate with half of the beam on the MgF_2 coating and half off. This is the first element of the optical system shown in Fig. 1. The beam is then elongated with a cylindrical lens in the direction along the dark line to make an elliptical TEM_{01} beam which is focused onto the atoms. A CCD image of the focus is shown in Fig. 2 along with a profile in the narrow direction. The TEM_{01} beam shown has a waist radius of $125\,\mu$m in the axial direction which is much longer than the BEC region to provide a rela-

#6677 - $15.00 US Received 28 February 2005; revised 30 March 2005; accepted 30 March 2005

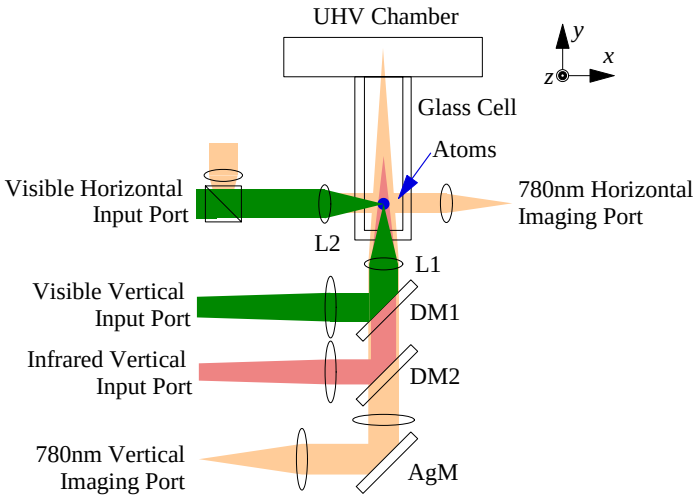

Fig. 3. Optical trap beam input ports and imaging ports in the science chamber are shown in this schematic. The setup has the capacity to accept vertical and horizontal visible beams as well as a vertical infrared beam. There are 780 nm absorption imaging beams for both vertical and horizontal diagnostics. L1 and L2 are the final lenses in the vertical and horizontal beam paths, DM1 and DM2 are dichroic mirrors, AgM is a silver mirror. Gravity in the figure is in the $-y$ direction.

tively uniform trap. The figure shows a fit to the ideal intensity profile of a TEM_{01} given in Eq. (1) which results in $W_x = 1.8\,\mu$m. It is noted that the measured profile fits that of an actual TEM_{01} beam very well which justifies our use of the simple formula given by Eq. (1) for calculations relating to the properties of the trap itself.

3.2. Experimental setup

For production of Bose-Einstein condensates, we have designed an experimental setup which consists of a double magneto-optic trap (MOT) system contained in an ultra-high vacuum chamber with upper and lower MOT regions separated by a differential pumping tube. The upper MOT is a six beam vapor cell MOT including an additional push beam which allows for loading of the lower MOT [16]. The lower MOT is contained by a custom 30 mm × 30 mm × 115 mm (outer) rectangular fused silica glass cell with 5 mm thick walls. The glass cell is an ultra-high vacuum region (UHV) and is the location for all experiments. Surrounding the glass cell is a Quadrupole Ioffe Configuration (QUIC) Magnetic Trap [17]. The experiment begins when order 10^9 ^{87}Rb atoms are loaded into the lower MOT in about 20 s and transferred into the quadrupole trap. The Ioffe coil is ramped on to move the atoms into a Ioffe-Prichard type magnetic trap. The trap center is offset from the lower MOT region by about 7.5 mm. The atoms are then cooled via forced RF evaporative cooling for about 20 s. This procedure produces an atom cloud of $N \approx 2 \times 10^6$ ^{87}Rb atoms near condensation. The cloud is then transferred adiabatically into a symmetric 20 Hz magnetic trap in the glass cell center by ramping down the current in the quadrupole coils while keeping the Ioffe coil current high. Placing the atoms back in the center of the glass cell allows for good optical access for the optical trap beams and for imaging of the atoms.

The beam interaction and imaging region of the setup is shown in Fig. 3. The setup includes

#6677 - $15.00 US Received 28 February 2005; revised 30 March 2005; accepted 30 March 2005

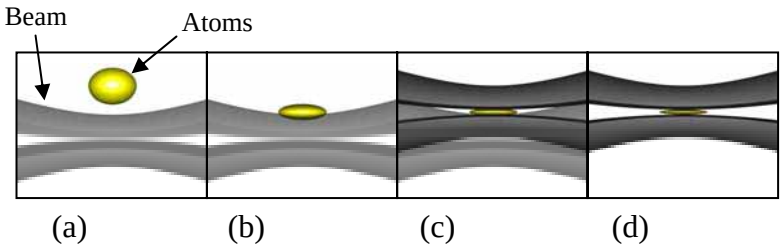

Fig. 4. Loading sequence of $hTEM_{01}$ trap. The pair of lobes for each $hTEM_{01}$ beam are represented in gray; the lower $hTEM_{01}$ is the ligher shade. The vertical infrared beam is not shown, but present in all (b) to (d). (a) Combined optical and magnetic trap. (b) Combined gravito-optical trap where the lower $hTEM_{01}$ beam acts as a sheet supporting against gravity. This trap has vertical trap frequency $\omega_y \cong 850\,\mathrm{Hz}$. (c) Transfer step into $hTEM_{01}$ beam. (d) Final optical trap inside $hTEM_{01}$ beam. This trap has vertical trap frequency $\omega_y \cong 21\,\mathrm{kHz}$.

horizontal and vertical input ports for visible light, which are used for our TEM_{01} beams. There is also an input port for a vertical infrared beam which is used for a radial confinement beam. The lenses L1 and L2 provide the final focusing of the optical trap beams. The optical trap we are describing here consists of a horizontally oriented TEM_{01} beam ($hTEM_{01}$) which will support the atoms against gravity and a vertical infrared beam of circular gaussian profile which provides a weak radial confinement [18]. The trap involves several configurations which allow for loading of atoms into the $hTEM_{01}$ node.

3.3. Method to load the optical trap

After initial preparation, atoms in the symmetric 20 Hz magnetic trap in the glass cell center may be transferred into the $hTEM_{01}$ beam by the steps shown pictorially in Fig. 4. It is not possible to directly capture the atoms into the $hTEM_{01}$ beam because the node spacing is only a few micrometers, but the size of the initial cloud is of order 200 μm. The steps are as follows: (a) The $hTEM_{01}$ beam is ramped on below the magnetically trapped atoms and the vertical infrared beam (not shown in Fig. 4) is turned on to provide a weak radial confinement of 60 Hz. (b) The center of the magnetic trap is moved below the $hTEM_{01}$ beam which now acts as a sheet against which the atoms are pressed. This increases the collision rate high enough for evaporation. The magnetic trap is ramped off while the atoms evaporate radially out of the infrared trap. This produces a condensate of up to 3×10^5 atoms. The atoms remain in a pancake shaped configuration pressed against the sheet by gravity. (c) The atoms are now captured inside another $hTEM_{01}$ which is ramped on in 200 ms, 4 μm above the lower one. (d) The lower $hTEM_{01}$ beam is then ramped off and the $hTEM_{01}$ beam containing the atoms is ramped up to full power.

The pair of $hTEM_{01}$ beams just discussed are actually both multiplexes of the same beam. The basic idea here is to use a multiple frequency acousto-optic modulator (AOM) [19] to produce several spots controlled independently with the driving radio frequency (RF). Such an AOM is driven with multiple frequencies of the form $P_{\mathrm{ac}} = \sum_{i=1}^{N} P_i \sin^2 2\pi\nu_i t$. In this case, $N = 2$ and each signal is generated by an RF synthesizer and combined with an RF power combiner. Each frequency produces a distinct first order diffraction angle. When imaged this leads to N spots which have spacing determined by the difference in drive frequency and intensity by the RF power at each frequency. This method allows for precise control of the positions

#6677 - $15.00 US Received 28 February 2005; revised 30 March 2005; accepted 30 March 2005

and intensities of the spots relative to each other and provides a powerful tool for condensate manipulation.

3.4. Final trap results

After the final trap configuration, the atoms are released suddenly and allowed to fall. During this time, the cloud shows a change of aspect ratio which indicates that the cloud had crossed the BEC transition in the trap [22]. The atom clouds are observed destructively with absorption imaging. This involves a 30 μs exposure with a resonant (780 nm) laser which is imaged onto a CCD camera. Under the assumption that the wavefunction in the strongly confined direction is Gaussian — that of the harmonic oscillator ground state [20], the cloud image may be fit and vertical size characterized by σ_y. The rate of vertical expansion in this case depends on the trap frequency in that direction as in

$$\sigma_y(t) = \sqrt{\frac{2\hbar}{m\omega_y}}(1+t^2\omega_y^2)^{1/2}. \tag{6}$$

Condensates in a high frequency trap exhibit a much larger rate of expansion in this direction. Fig. 5 shows expansion of atoms from a hTEM$_{01}$ trap. The beam used in this case had parameters: $W_y = 2.4$ μm, $W_z = 125$ μm, and $P = 1.0$ W with wavelength $\lambda = 532$ nm, from which Equations 3 and 4 give [23] a trap depth of $U_0/k_B = 93$ μK and a trap frequency of $\omega_y/2\pi = 21$ kHz. The spontaneous scattering rate may be estimated from Eq. (5) at the harmonic oscillator length $a_q = 75$ nm, which results in $R(a_q,0) \cong 6\times10^{-3}\,\mathrm{s}^{-1}$ per atom, meaning that there are few total events over the time of the experiment compared to the BEC population. The line fit in Fig. 5 indicates a trap frequency of 24 ± 4 kHz, consistent with calculations. The trap frequencies of the hTEM$_{01}$ trap are made high due in part to the tight focus obtained with $W_y = 2.4$ μm. Because of the slightly better $f/\#$ of L1 [24] over L2 in Fig. 3, a vertical TEM$_{01}$ (vTEM$_{01}$) in our system can obtain even tighter focus as in Fig. 2. The largest trap frequency we have observed in our system with this method is 66 ± 7 kHz, which has been for this vTEM$_{01}$ beam with $W_x = 1.8$ μm, $W_z = 125$ μm, and $P = 3.7$ W. By loading a condensate into a crossed TEM$_{01}$ (xTEM$_{01}$) trap consisting of both the hTEM$_{01}$ and vTEM$_{01}$ mentioned here, it is possible to create a one-dimensional BEC [25].

4. Comments on the optical trap

The hTEM$_{01}$ trap alone produces a two-dimensional condensate. The wavefunction of the condensate may be written assuming a Gaussian profile in the strongly confined direction and a Thomas-Fermi shape in the radial directions [21]. In the strongly confined direction, the atoms occupy the single particle ground state energy level with value $\hbar\omega_q/2$, where $2\pi\hbar$ is Planck's constant. The trap frequency, calculated from Eq. (4), is that for the center of the trap. Spatially, the trap frequency has a radial dependence $\omega_q = \omega_q(p,s)$ which implies a spatial ground state energy shift. This dependence is due to the Gaussian beam profile along the p axis and the $W_{q,p}^2$ dependance on propagation distance s, see note [12]. The result is a weak potential of the form $m\omega_p^2 p^2/2$ and $m\omega_s^2 s^2/2$ in these directions. The radial trap frequencies may be written as

$$\frac{\omega_p}{2\pi} = \frac{i}{\sqrt{2}\pi}\frac{1}{W_p W_q^{1/2}}\left(\frac{e\hbar^2 U_0}{m^3}\right)^{1/4}, \tag{7}$$

and

$$\frac{\omega_s}{2\pi} = \sqrt{\frac{3}{2}}\frac{i}{2\pi^2}\frac{\lambda}{W_q^{5/2}}\left(\frac{e\hbar^2 U_0}{m^3}\right)^{1/4}, \tag{8}$$

#6677 - $15.00 US Received 28 February 2005; revised 30 March 2005; accepted 30 March 2005

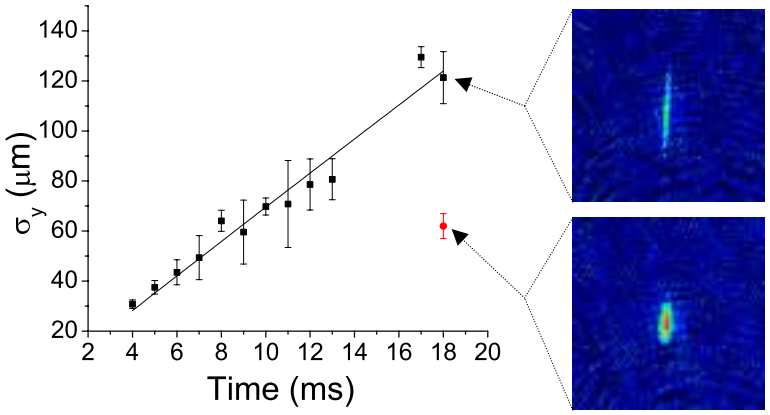

Fig. 5. BEC Expansion from hTEM$_{01}$ trap. The black squares give data points for σ_y as a function of time for condensates released at time zero. The data is consistent with the 21 kHz expected trap frequency for this TEM$_{01}$ trap. The images to the right are absorption images of one of the shots of the indicated data point. The upper picture is of a condensate released from the inside the TEM$_{01}$ trap, and the lower was released from above the sheet (the gravito-optical trap) as in Figure 4(b). This is the red circle data point on the plot. The lower picture is a 3-D condenstate and does not obey Equation 6.

where the approximation $(W_q/W_p)^4 \ll 1$ was used in deriving Eq. (8). These imaginary oscillation frequencies each represent an anti-trapping potential. For the $\omega_q/2\pi = 21$ kHz hTEM$_{01}$ trap discussed above, these anti-trapping frequencies are $\omega_p/2\pi = 12i$ Hz and $\omega_s/2\pi = 40i$ Hz. The vertical infrared beam which provides a weak radial confinement of 60 Hz over compensates this effect and radially traps the atoms. In the case mentioned using a xTEM$_{01}$ configuration for a one-dimensional trap [25], $\omega_s/2\pi$ plays no role because of the geometry and only the tiny $\omega_p/2\pi$ is an issue.

Here in lies a major advantage of the TEM$_{01}$ trap over other blue traps, for example, a blue Gaussian sheet pair each with power $P/2$. When the sheets are separated in q by $\sqrt{3}W_q$, they have an optimum trap frequency given by

$$\frac{\omega_q'}{2\pi} = \frac{1}{\mathrm{e}^{3/4}}\sqrt{\frac{\mathrm{e}U_0}{\pi^2 m W_q^2}}, \tag{9}$$

similar to Eq. (4) but reduced by a factor of $\mathrm{e}^{-3/4} \approx 0.47$. In addition to having a lower trapping frequency in the strong direction, these traps have much larger anti-trapping frequencies. In contrast to the TEM$_{01}$ trap which has a zero intensity profile along the p axis at $q = 0$, this trap has a Gaussian axial intensity profile which produces an anti-trap in addition to the weak ground state shift anti-trap described above. These effects result in trap frequencies

$$\frac{\omega_{p(1)}'}{2\pi} = \frac{i}{\sqrt{2}\mathrm{e}^{3/4}}\sqrt{\frac{\mathrm{e}U_0}{\pi^2 m W_p^2}} \quad \text{and} \quad \frac{\omega_{p(2)}'}{2\pi} = \frac{i}{\sqrt{2}\pi\mathrm{e}^{3/8}}\frac{1}{W_p W_q^{1/2}}\left(\frac{\mathrm{e}\hbar^2 U_0}{m^3}\right)^{1/4}, \tag{10}$$

where $\omega_{p(1)}'/2\pi$ is due to the axial intensity profile and $\omega_{p(2)}'/2\pi$ the ground state shift. These add in quadrature to give the overall $\omega_p'/2\pi$. The first does not exist for the TEM$_{01}$ trap and is the larger effect. The second corresponds with Eq. (7). Using the same parameters as the

#6677 - $15.00 US Received 28 February 2005; revised 30 March 2005; accepted 30 March 2005

hTEM$_{01}$ trap above, this double Gaussian trap has trap frequencies $\omega_q'/2\pi = 9.8\,\mathrm{kHz}$ and $\omega_p'/2\pi = 132i\,\mathrm{Hz}$. That is, this trap has less than half the trap frequency in the q direction and more than an order of magnitude larger anti-trapping frequency in the p direction.

It is worth noting that a blue trap with a dark trapping region as presented here has several advantages over a red trap [14]. A red trap produces an attractive potential where the atoms are high field seeking. This results in a larger spontaneous scattering rate. Because red traps use longer wavelength light, they are also more limited in focus size — this is critical for obtaining very high trap frequencies. An additional limitation is the depth of the traps produced. If one imagines using a single red sheet to produce a condensate as described for our hTEM$_{01}$ trap, it is clear that the red trap will have an attractive potential in the radial directions. Because the trap is so deep, evaporative cooling is difficult.

Recent work with a blue TEM$_{01}$ beam combined with a magnetic trap has produced quasi-2D condensates [26]. In their experiment, the authors operate in a regime where the focus in both q and p directions is much larger than in the case presented here. Because of the longer depth of focus and larger W_p used in their experiment, the optical trap has a more uniform potential. This is a preferred regime in which to operate for the study of vortex dynamics in two-dimensions, for example, as the authors point out. The central trap frequencies, however, obtained are considerably smaller: by a factor of 10 for the hTEM$_{01}$ trap and a factor of 30 for vTEM$_{01}$ trap than in the case presented here. For the possibility of entering regimes of quantum gases as mentioned earlier [6, 7, 8, 9, 10], such trapping strengths are required.

5. Conclusions

We have proven a method to create TEM$_{01}$ beams with a holographic plate and provided a method for loading a BEC into the tightly confined TEM$_{01}$ trap. This method pushes the possibilities of making single lower dimensional condensates. The trapping strengths which have been obtained in these single site optical traps are comparable to those often obtained in optical lattices. This technique paves the way towards experiments with single highly confined condensates.

Acknowledgments

The authors would like to acknowledge support from the NSF, the R.A. Welch Foundation, discussions with A.M. Dudarev and G. Price. T.P.M. acknowledges support through the NSF Graduate Research Fellowship and F.S. through the Alexander von Humboldt Foundation.

#6677 - $15.00 US Received 28 February 2005; revised 30 March 2005; accepted 30 March 2005